Supporting Information for

Transition from reconstruction towards thin film on the (110) surface of strontium titanate

Z. Wang*[,1], A. Loon[2], A. Subramanian[2], S. Gerhold[1], E. McDermott[3], J. A. Enterkin[4], M. Hieckel[1], B. C. Russell[5], R. J. Green[6], A. Moewes[6], J. Guo[7], P. Blaha[3], M. R. Castell[5], U. Diebold[1], and L. D. Marks[2]

[1]Institute of Applied Physics, TU Wien, Wiedner Hauptstrasse 8-10/134, 1040 Vienna, Austria
[2]Department of Materials Science and Engineering,
Northwestern University, Evanston, IL 60208, USA
[3]Institute of Materials Chemistry, Vienna University of Technology, Getreidemarkt 9/165-TC, 1060 Vienna, Austria
[4]Department of Chemistry,
Northwestern University, Evanston, IL 60208, USA
[5]Department of Materials, University of Oxford,
Parks Road, Oxford OX1 3PH, UK
[6]Department of Physics and Engineering Physics, University of Saskatchewan,
116 Science Place, Saskatoon, SK S7N 5E2, Canada
[7]Beijing National Laboratory for Condensed Matter Physics and Institute of Physics, Chinese Academy of Sciences, Beijing 100190, People's Republic of China

* Email: zhiming.wang@psi.ch

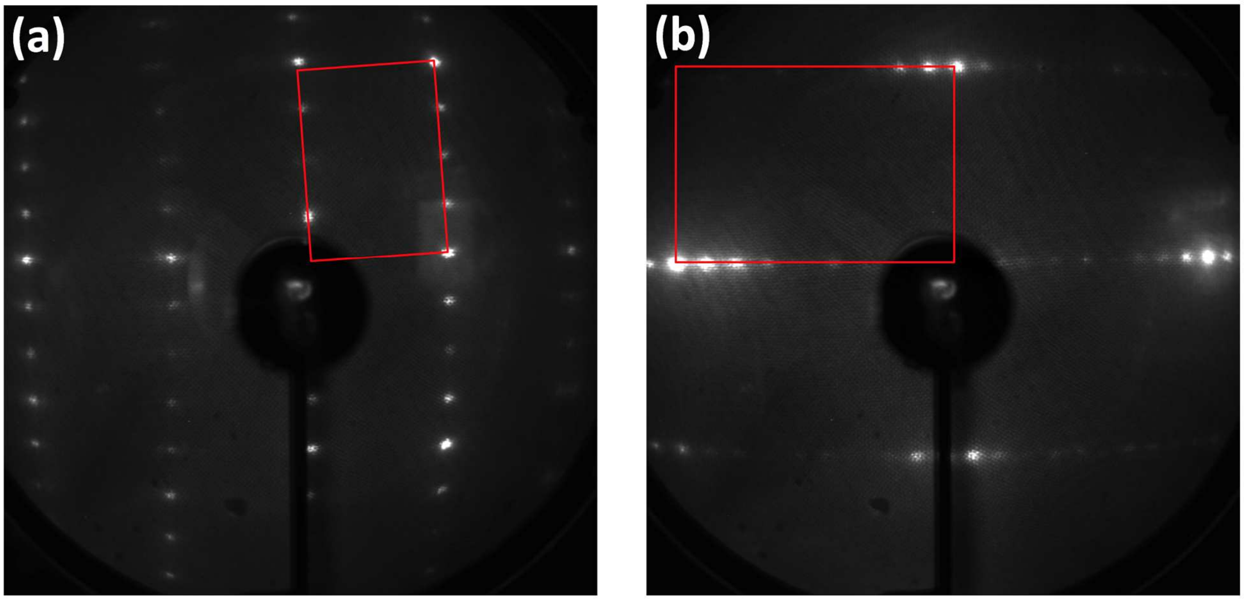

Supplemental Figure S1, showing LEED patterns of in (a) the 4×1 reconstruction and in (b) the n×5 reconstruction, with the 1×1 unit cell shown in red in both. Due to the much higher background in LEED compared to TED, as well as the much more dynamical nature of the scattering it is not clear in (b) whether it is a 1×5 or a 2×5 surface; as shown later in Supplemental Figure S5 and discussed in the main text the additional scattering from the "2" periodicity is weak due to disorder.

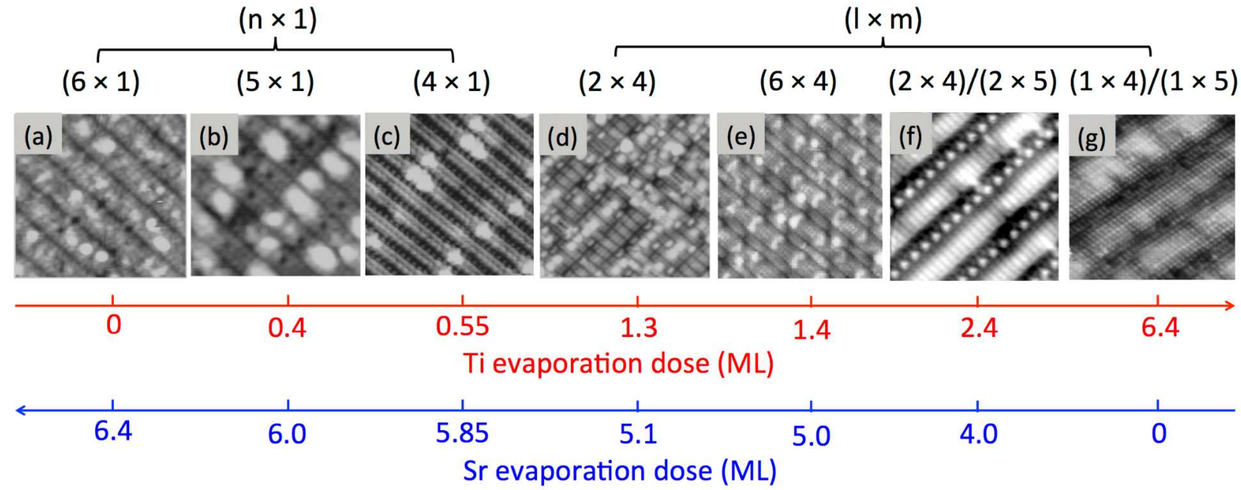

Supplemental Figure S2: (a-g) Map of the observed structures as a function of dosing of either Sr or Ti on the $SrTiO_3$ (110) surface, showing more involved, probably metastable, 2×4 and 6×4 structures. Note that the x-axis gives evaporation doses rather than coverage, which could be different due to diffusion of surface atoms into the bulk.

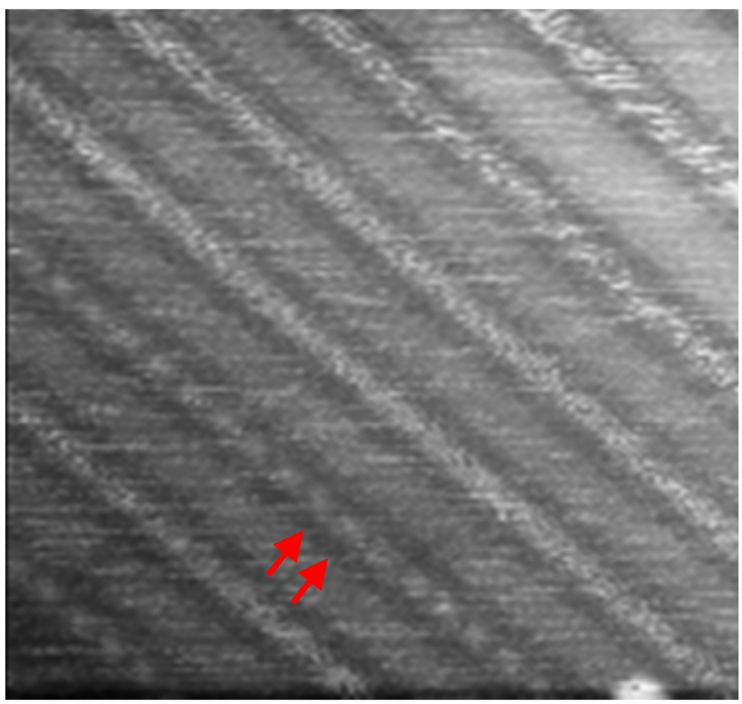

Supplemental Figure S3: STM image showing co-existing regions of (0,0,2) periodicity arrowed in an otherwise (0,0,1) periodicity.

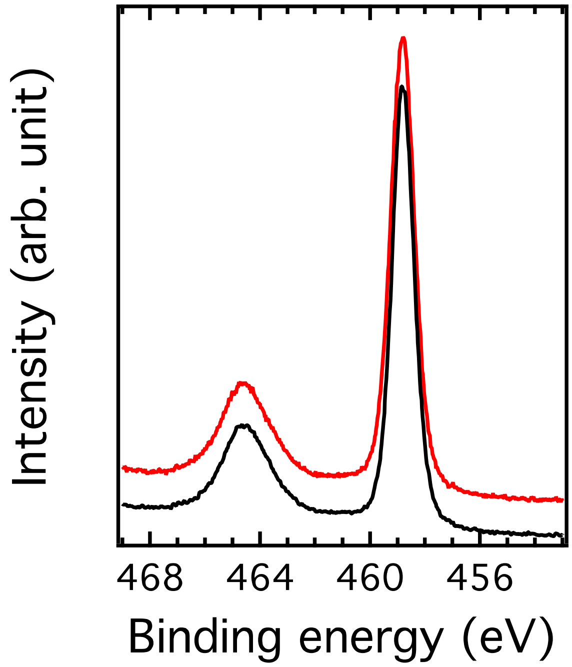

Supplemental Figure S4: Ti 2*p* core-level photoemission spectra for the (4 × 1) (black curve) and (2 × 5) (red curve) reconstructed surfaces. The Ti valence is 4+ for both surfaces. The spectra are aligned and measured with photon energy of 605 eV at grazing angle.

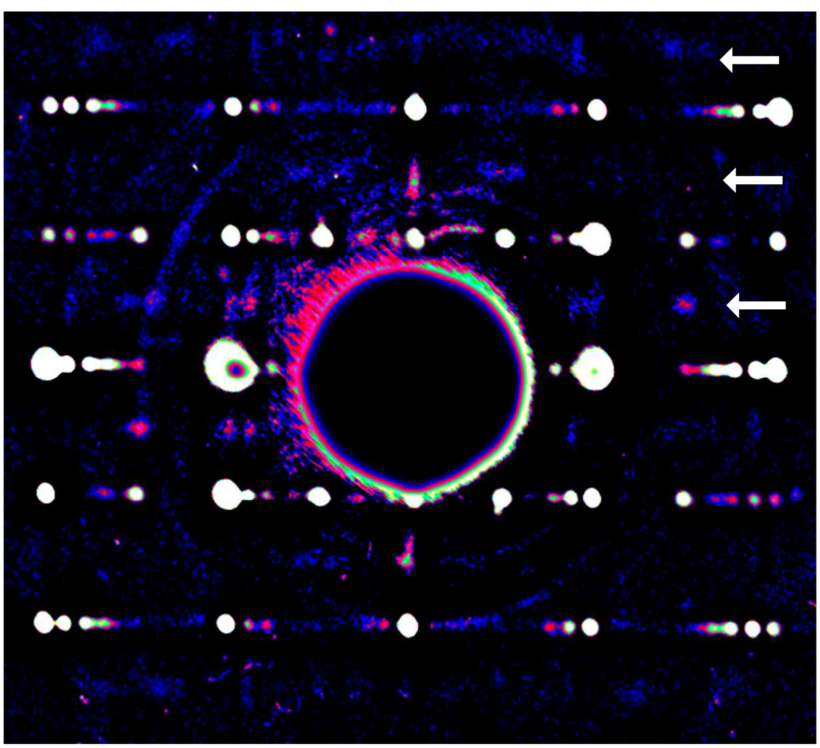

Supplemental Figure S5: Pseudocolor representation of a high-pass filtered diffraction pattern of a 2×4 sample. In addition to the strong intensities of the 1×4 lattice, there is weak intensity correlating with a statistically disordered 2×4 superlattice, arrowed.

Table S1: Experimental intensities and calculated intensities using Shelx for the 2×4 electron diffraction data using a kinematical model with occupational disorder.

H	K	Iobs	Icalc
3	3	58.69	61.37
2	6	99.63	124.41
3	6	31.16	91.2
1	7	287.76	248.97
2	7	91.72	101.18
4	10	35.44	33.79
3	11	63.07	59.64
4	11	59.44	46.8
1	13	72.11	71.65
2	13	109.61	72.86
4	13	24.11	89.24
0	14	360.47	372.52
1	14	53.92	62.78
2	14	177.06	171.9
4	14	43.46	43.93
0	15	841.4	890.74
1	15	80.94	58.6
2	15	431.31	488.2
3	15	24.23	51.45
4	15	106.42	89.87
0	17	64.16	65.68
4	18	162.92	104.76
0	19	62.49	62.7
1	19	61.85	65.21
0	21	40.61	74.72
2	22	84.35	56.02
2	23	128.22	118.68
3	23	1.49	44.91
1	26	0.51	51.67
2	26	0.28	58.18
1	29	38.48	48.51

Table S2: Experimental intensities and calculated intensities using Shelx for the 2×5 electron diffraction data using a kinematical model with occupational disorder.

H	K	Iobs	Icalc
1	2	472.96	395.63

3	2	65.67	97.57
1	3	131.45	125.42
2	3	92.79	365.18
3	3	20.64	162.36
1	4	286.63	213.69
2	4	76.25	257.67
3	4	51.58	52.23
2	6	9.82	207.7
3	6	59.38	55.09
1	7	52.73	131.18
2	7	101.81	179.53
0	8	129.67	379.13
1	8	256.9	339.86
2	8	38.48	211.07
3	8	81.32	174.62
0	9	794.39	552.22
1	9	1483.67	1276.86
2	9	222.53	292.65
3	9	257.23	455.64
1	12	233.43	103.16
2	12	370.19	161.19
3	12	62.2	116.23
0	13	377.21	273.44
1	13	265.06	164.55
2	13	174.82	243.11
1	14	113.94	125.41
2	14	14.7	194.71
3	14	37.78	80.24
0	16	345.04	334.51
1	16	93.59	84.72
2	16	180.97	161.17
3	16	35.16	49.7
0	17	704.56	850.27
1	17	155.24	147.37
2	17	387.72	350.93
3	17	58.54	745.76
0	18	1293.38	1535.41
1	18	166.37	121.64
2	18	736.46	700.02
3	18	68.84	81.34
0	19	3710.21	5040.02

1	19	213.31	246.48
2	19	2184.5	2379.52
1	21	79.84	73.14
2	21	151.99	78.1
0	22	222.85	138.72
1	22	77.69	209.62
0	23	97.81	253.09
1	23	90.54	89.75
2	23	66.38	137.92
1	24	80.12	77.79
2	24	129.79	100.23
0	26	349.96	192.53
1	26	69.78	108.3
0	27	70.15	52.81